

1 Towards a Pixel TPC part II: particle identification
2 with a 32-chip GridPix detector

3 M. van Beuzekom^a, Y. Bilevych^b, K. Desch^b, S. van Doesburg^a,
4 H. van der Graaf^a, F. Hartjes^a, J. Kaminski^b, P.M. Kluit^a,
5 N. van der Kolk^a, C. Ligtenberg^a, G. Raven^a, J. Timmermans^a

6 ^a*Nikhef, Science Park 105, 1098 XG Amsterdam, The Netherlands*

7 ^b*Physikalisches Institut, University of Bonn, Nussallee 12, 53115 Bonn,*
8 *Germany*

9 **Abstract**

10 A Time Projection Chamber (TPC) module with 32 GridPix chips was con-
11 structed and the performance was measured using data taken in a test beam
12 at DESY in 2021. The analysed data were taken at electron beam momenta
13 of 5 and 6 GeV/c and at magnetic fields of 0 and 1 Tesla(T). Part I of the
14 paper has described the construction, setup and tracking results.

15 The dE/dx or dN/dx resolution for electrons in the 1 T data per meter
16 of track length with 60% coverage was measured to be 3.6% for the dE/dx
17 truncation method and 2.9% for the template fit method using the successive
18 distances between the hits.

19 The single electron efficiency at high hit rates was studied. For hit rates
20 up 1.4 kHz per chip a reduction of at most 0.6% in the relative efficiency was
21 measured.

22 Hit bursts due to highly ionising particles were characterized.

23 The resolution in the precision plane as a function of the incident track
24 angle was measured in the $B = 1$ T data using reconstructed circle tracks.

*Corresponding author, Telephone: +31 20 592 2000
Preprint submitted to Nuclear Instruments and Methods A
Email address: s01@nikhef.nl (P.M. Kluit)

25 The resolution in the precision plane is - as expected - independent of the
26 incident angle ϕ within an uncertainty of $16 \mu\text{m}$.

27 The projected particle identification (PID) performance of a GridPix
28 Pixel TPC in the proposed ILD experiment at a future ILC e^+e^- collider
29 was presented using the $B=1$ T test beam results for the measured electron
30 PID resolution. The expected pion-kaon PID separation for momenta in the
31 range of 2.5-45 GeV/c at $\cos\theta = 0$ is more than $5.5(4.5)\sigma$ for the template
32 fit (dE/dx truncation) method.

33 *Keywords:* Micromegas, gaseous pixel detector, micro-pattern gaseous
34 detector, Timepix, GridPix, pixel time projection chamber

35 1. Introduction

36 As a step towards a Pixel Time Projection Chamber for a future collider
37 experiment [1], [2], a module consisting of 32 GridPix chips based on the
38 Timepix3 chip was constructed. The GridPix chips have a very fine granu-
39 larity of 256×256 pixels of $55 \times 55 \mu\text{m}^2$ and a high efficiency about 85% to
40 detect single ionisation electrons.

41 The 32-GridPix chip detector was put in a test beam at DESY and com-
42 plemented with two sets of Mimosas26 silicon detector planes. The analysed
43 data were taken at electron beam momenta of 5 and 6 GeV/c and at magnetic
44 fields of 0 and 1 T.

45 A description of the construction of the GridPix TPC module, the test
46 beam setup and data taking conditions can be found in part I of our paper
47 [3]. The paper explains the track reconstruction procedure and the precise
48 TPC tracking results that were obtained.

49 In the following sections the analysis results for different topics will be
50 presented. Firstly, the particle identification performance using dE/dx or
51 dN/dx will be measured. Secondly, the single electron efficiency at high
52 hit rates will be determined. Thirdly, the characterisation of large hit bursts
53 caused by highly ionising particles will be presented. Fourth, the resolution in
54 the precision plane as a function of the incident track angle will be measured.
55 Finally, the projected particle identification performance for a Pixel TPC in
56 the proposed ILD experiment at ILC [4] will be presented and discussed.

57 **2. Particle Identification using dE/dx or dN/dx**

58 Particles can be identified by their characteristic energy loss per unit
59 of track length dE/dx loss and/or the number of primary clusters dN/dx
60 produced along the track. In a GridPix detector one can measure the number
61 of hits produced along the track and their relative distance.

62 The distribution of the number of TPC track hits per chip for the $B = 0$
63 T and for the $B = 1$ T data sets are a starting point for a measurement of
64 the dE/dx or dN/dx performance. As was discussed in part I of the paper
65 [3], the mean number of hits is measured to be 124 and 89 in the $B = 0$ T
66 and 1 T data sets respectively. The most probable values are respectively 87
67 and 64.

68 In order to measure the track performance of dE/dx or dN/dx , a track
69 selection was applied selecting tracks crossing the central chips - defined in
70 [3]. The individual chips were calibrated to give the same mean number of
71 hits per chip. By combining the hits associated to the track from several
72 events, a new 1 m long track was formed. The 1 m long track has a coverage

73 of 60% because inactive regions (chip edges and e.g. guard) were included.

74 By applying different analysis methods, the dE/dx or dN/dx resolution
75 can be measured from data.

76 Both methods project the hits along the track in the xy plane. This gives
77 a distribution of hits as a function of the distance along the track in pixels.
78 The first method rejects large multi-electron clusters with more than in total
79 6 hits in 5 consecutive pixel bins. Finally, a dE/dx truncation at 90% is
80 performed using samples of 20 pixels; so the 10% largest dE/dx values are
81 removed and dE/dx re-estimated. This method does not fully exploit the
82 full granularity of the pixel TPC.

83 The second method exploits the distribution of the minimum distance
84 between consecutive hits in the xy precision plane. If only single electron
85 clusters were produced in a gas, one would expect an exponentially falling
86 distance distribution. Multi-electron clusters will give rise to a peak at low
87 distances that is smeared out by the transverse diffusion process. The slope
88 of the exponential distribution is proportional to the dN/dx i.e. the clusters
89 produced by the traversing beam electron. The long Landau tail in the
90 dE/dx distribution is coming from the multi-electron clusters that will peak
91 at low distances.

92 Using a large number of tracks, it is possible to measure from data the
93 shape of the minimum distance distribution. At distances above approx-
94 imately 10 pixels the distribution follows an exponential distribution. At
95 lower distance, weights for the $B=0$ T and 1 T data are determined and
96 applied to ensure an exponential distribution over the whole range.

97 Finally, per 1 m of track length track, a fit to the distance distribution in

98 data is performed with the following template function:

$$N(d_{xy}) = N_0 \text{weight}(d_{xy}) e^{-\text{slope} d_{xy}}. \quad (1)$$

99 where d_{xy} is the minimum distance of the hits in the precision plane (xy).
100 The slope and N_0 - normalisation - are left free in the per track fit, the
101 weights for the $B = 0$ and 1 T data are fixed using the whole data set.

102 The test beam data provide a dE/dx or dN/dx measurement for electrons.
103 The data were also used to perform a measurement of the response of a
104 minimum ionising particle (MIP) - here defined as a particle that produced
105 70% of the electron dE/dx . By dropping 30% of the hits associated to
106 the track and applying the two methods, the response of a MIP could be
107 measured and the linearity of the methods tested.

108 The relative resolution is defined as the r.m.s. of the distribution divided
109 by the mean and the results are shown in Table 1. The resolution of the $B =$
110 1 T data is about 40% better than the $B = 0$ T data. This is consistent with
111 the smaller fluctuations that are present in the distributions of the number
112 of hits per chip in the $B = 1$ T data [3]. The template fit method has in the
113 $B = 1$ T data a 20% better performance than the dE/dx truncation method.
114 One might argue that with more diffusion the results from the template fit
115 method will move more towards the results of the dE/dx truncation method.
116 Note however that the diffusion contribution to the track resolution in the
117 1 T data is already sizeable compared to the pixel size and varies between
118 85-150 μm .

119 The results for the 1 T data are shown in Figure 1 for electrons and MIPs
120 for the dE/dx truncation and template fit methods. The unit of the fitted
121 slope is inverse (pixel) distance, as is clear from the formula in Eq. 1. The

Table 1: dE/dx or dN/dx resolution for different methods and data sets

Method	$B= 0$ T [%]	$B= 1$ T [%]
dE/dx truncation	6.0	3.6
template fit	5.4	2.9

122 linearity - defined as the mean MIP response divided by the mean electron
 123 response divided by 0.7 - was measured to be 1.03 for method 1 and 1.07
 124 for method 2. This value is slightly different from 1, and can be corrected
 125 for by scaling the expected values for different particles as a function of the
 126 measured momentum.

127 The dE/dx or dN/dx result of the 32-chip GridPix detector for electrons
 128 is impressive. It has currently, the best resolution per meter of track length
 129 of constructed TPCs running at atmospheric pressure - and demonstrates
 130 the particle identification capabilities of a GridPix Pixel TPC.

131 sectionSingle electron efficiency at high hit rates

132 The efficiency of the GridPix device to detect a hit in a high (low) rate
 133 environment is measured comparing the mean time over threshold (TOT) for
 134 low and high rate runs at B fields of 0 and 1 T. The mean TOT is sensitive
 135 to the single electron efficiency of the detector. In order to extract a precise
 136 result, hits associated to TPC tracks were used. The track selection is the
 137 same as in section 2. The analysed runs for the $B = 0$ T data set were runs
 138 6916, 6934 and 6935 and for the $B = 1$ T data set runs 6969 and 6983.

139 For each run the mean TOT values were measured in the interval between
 140 0.15 and 1.4 μ s. These cuts were applied to remove the noise and the upper
 141 tail of the distribution.

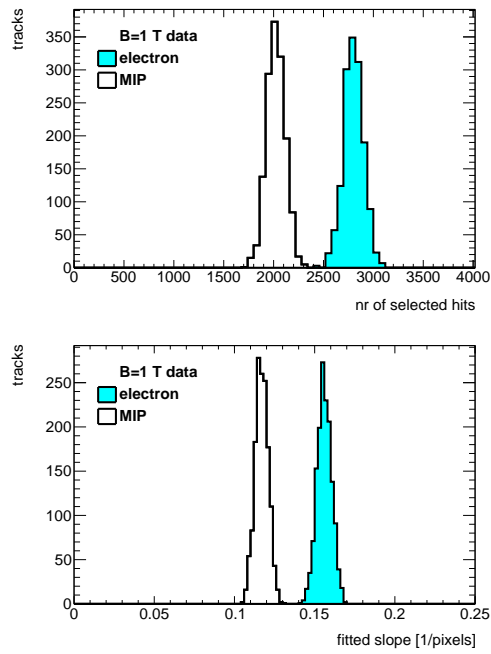


Figure 1: Distribution of the number of selected hits for the dE/dx truncation method (left) and the fitted slope for the template fit method (right) for an electron (light blue shaded) and for a MIP using 1 m long tracks with 60% coverage for the $B = 1$ T data.

Table 2: Mean TOT and rates for different runs

run	B	TOT1	TOT2	triggers	run time	Hits1	Hits2	trig rate	Rate1	Rate2
	T	μs	μs	10^3	10^3s	10^6	10^6	Hz	hits/s	hits/s
6916	0	0.628	0.653	16.8	23.2	6.25	13.1	0.72	269	565
6934	0	-	0.651	7.34	2.41	-	20.5	30.4	-	8479
6935	0	0.620	-	7.39	2.41	6.95	-	30.6	2878	-
6969	1	0.650	0.666	7.94	13.8	1.93	2.16	0.57	139	156
6983	1	0.657	0.678	6.79	2.83	11.6	14.1	24.1	4110	4986

142 The results for the measured average TOT for different runs and hit
143 rates are summarised in Table 2. TOT1(2) denotes the mean TOT for upper
144 and lower half (in x) of the module and Hits1(2) corresponds to number
145 of recorded raw hits. The mean Rate1(2) was calculated dividing the total
146 number of raw hits by the total run time. For the $B = 0$ T data, two high
147 rate runs 6934 and 6935 taken at a beam momentum of 5 GeV/c had to be
148 analysed because the beam crossed either the upper or the lower part of the
149 module and therefore no measurement could be performed (denoted by -).
150 The statistical uncertainties are negligible.

151 The relative change in the mean TOT for the $B = 0$ data is -1.2% (upper)
152 and -0.3% (lower). In this case the rate goes up to 8.5 kHz for 6 chips or 1.4
153 kHz per chip. The relative change in the mean TOT for the $B = 1$ T data
154 is +1% (upper) and +1.7% (lower) The rate goes up to 5 kHz for 6 chips or
155 1.2 kHz per chip.

156 The relative change in the mean TOT can be related to the relative change

157 in the single electron efficiency $\delta\epsilon/\epsilon$ by:

$$\delta\text{TOT}/\text{TOT} = d \delta\epsilon/\epsilon. \quad (2)$$

158 The derivative d is about 0.5 at the mean working point of $\text{TOT}=0.65 \mu\text{s}$
159 and is determined from the measured efficiency-TOT curve in [2].

160 This means that the relative efficiency is stable at the level of +0.9% (B
161 = 1 T) and -0.6% ($B = 0$ T) for hit rates up to 1.2 (1.4) kHz per chip. To
162 conclude, running at hit rates up 1.4 kHz per chip gives a reduction of at
163 most 0.6% in the relative efficiency.

164 **3. Characterisation of hit bursts**

165 In event displays hit burst caused by highly ionising particles (e.g. alpha
166 particles or delta electrons) can be observed. An example event in run 6969
167 is shown in figure 2. A large variety of hit patterns can be observed: large
168 radii (open) circles, smaller size radius circles from low momentum particles,
169 curlers and more confined bursts. A track with a momentum of 1 MeV/c
170 will have a typical radius of 121 pixels.

171 A Pixel TPC is well suited to study and characterize these typical hit
172 bursts. A pixel TPC also allows to improve the high momentum tracking by
173 removing these bursts.

174 To study the hit bursts, the data of run 6969 - taken at a 5 GeV/c beam
175 momentum in a $B = 1$ T field - were analysed. Bursts were selected with
176 more than 100 hits in a radius of 50 pixels around the burst centre within
177 a time window of 200 ns around the mean time. The mean position in xy
178 and the mean time of the burst were iteratively estimated. The bursts were

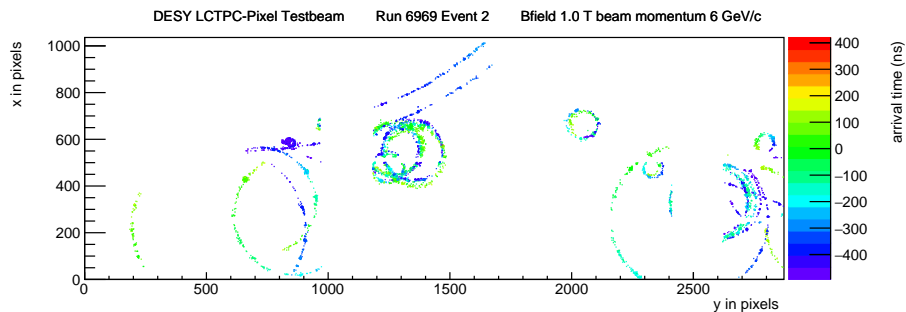


Figure 2: An event display for run 6969 event 2 taken at a 5 GeV/c beam momentum in a $B = 1$ T field. The hits are shown in the xy plane in colour the time of arrival is shown.

179 characterized by the number of associated hits, the radius in which 90% of the
 180 hits are found (radius90) and the time in which 90% of the hits are detected
 181 (time90). The stacked distributions for the radius90 and time90 variables for
 182 different burst sizes are shown in Figure 3.

183 It is clear that the radius90 and time90 distributions broaden as a function
 184 of the number of hits. In particular the time90 distribution develops a long
 185 tail for high number of hits. Note that hits that end up on the same pixel
 186 within the TimePix3 pixel dead time of 475 ns will not be recorded, so part
 187 of the core of the burst might remain undetected. Still the detector is able
 188 to record hit bursts of at most 7854 hits in a 50 pixel radius. The largest hit
 189 burst in run 6969 had 3180 hits.

190 For high momentum tracking it is important to cut tightly on the track
 191 residuals in xy and z . In particular the cut in z reduces the impact of bursts
 192 in the $B = 1$ T data. In the pattern recognition one could run a burst finding
 193 algorithm and down weight in the track fit the hits associated to bursts. This
 194 will remove biases and improve the track parameter estimation.

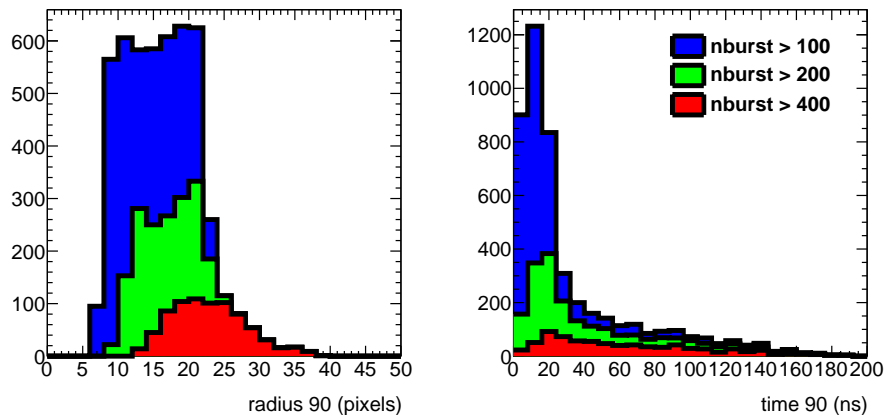


Figure 3: The stacked distributions for radius90 and time90 for burst with more than 100 (blue), 200 (green) and 400 (red) hits for run 6969.

195 4. Track resolution as function of the angle

196 The resolution in the precision plane as a function of the incident angle of
 197 the track will be measured in the $B = 1$ T data set. For a pad based readout
 198 system the resolution has a strong dependence on the incident angle see e.g.
 199 [5]. The resolution is best if the incident track angle is parallel to the strip
 200 direction.

201 For a GridPix pixel TPC - with squared pixels - the resolution is expected
 202 to be independent of the incident angle. In order to test experimentally
 203 this hypothesis, reconstructed circle tracks were selected. Examples of circle
 204 tracks can be observed in the event display shown in Figure 2. For circles, the
 205 incident ϕ angle of the track depends on the position of the individual hits
 206 on the circle in the xy plane. The range of ϕ angles depends on the radius.
 207 For radii smaller than 500 pixels a large ϕ range can be probed. Using the
 208 residuals in the xy plane, it is possible to measure the resolution of the hits

209 as a function of the incident ϕ angle of the track.

210 A dedicated pattern recognition program was written to find and fit mul-
211 tiple circles in an event. To find circles, large clusters were down weighted.
212 The hits within 15 pixels (in xy) of the chip edge were removed. In the circle
213 fit, the resolution in xy was estimated to be about 4 pixels and in z it was
214 1 mm. Outlier hits at more than 2.5 standard deviation were iteratively re-
215 jected. For the selection of circles it was required that the fit $\chi_{xy}^2/d.o.f.$ and
216 $\chi_z^2/d.o.f.$ was less than 5. Finally, the radius of the circle had to be larger
217 than 50 pixels (corresponding to a momentum cut of 0.4 MeV/c), at least
218 20 hits should lie on the circle. The total ϕ span of the selected hits on the
219 circle should be at least 1 rad. The hits with ϕ values below $\pi/8$ and above
220 $15\pi/8$ were removed.

221 The selected data set has 973 circles, with a mean radius of 155 pixels
222 and a mean number of hits of 194. Because the resolution depends on the
223 radius (i.e. the momentum) and small radii span a large phi range, the data
224 were re-weighted as a function of the circle radius. Finally, the resolution in
225 xy was extracted - using a Gaussian fit to the track residuals in the range
226 of $\pm 2\sigma$ around the centre. The fitted resolution in xy as a function of the ϕ
227 incident angle of track for the hits on the circle is shown in Figure 4.

228 A curve was fitted to the data using the following expression:

$$\sigma_{xy} = \sigma_0 + \sigma_1 \cos \phi, \quad (3)$$

229 where σ_0 and σ_1 were left free. The fit result yielded $\sigma_0 = 0.241$ mm and
230 $\sigma_1 = 0.016$ mm and describes the modulation observed in the data.

231 It can therefore be concluded that the resolution in the precision plane is
232 independent of the incident angle ϕ within an uncertainty of 16 μm .

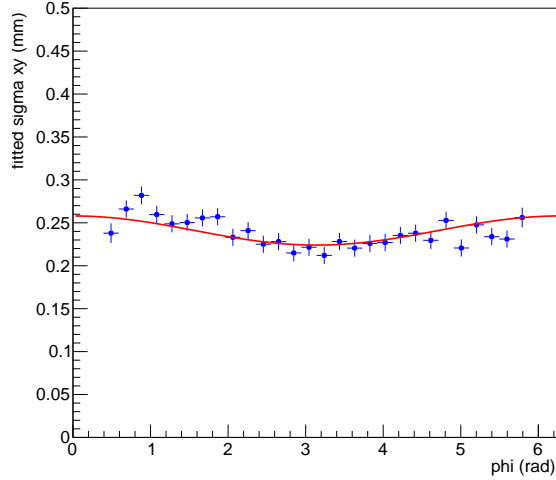


Figure 4: The fitted resolution in xy as a function of the ϕ incident angle of the hits on the circle. The fitted curve in red is given in Eq. 3.

233 *4.1. Projected particle identification performance for a Pixel TPC in the pro-*
 234 *posed experiment ILD at a future ILC*

235 The particle identification (PID) performance of electrons in the test
 236 beam for momenta of 5-6 GeV/c was measured to 2.9% for the template
 237 fit and 3.6% for the dE/dx truncation method at $B = 1$ T for 1 m long
 238 tracks with 60% coverage. The TPC of the proposed ILD detector [4] has
 239 an inner radius of 329 mm, an outer radius of 1770 mm and a half length
 240 of 2350 mm. In the ILD TPC this will correspond to an expected electron
 241 PID resolution of 2.4% (fit) and 3% (truncation) at polar angles of $\theta = \pi/2$
 242 ($\cos \theta = 0$) and a track length ($tlength_0$) of 1441 mm. The PID resolution
 243 for different particles can be written as:

$$\sigma_i = \sigma_e \sqrt{tlength_0 E_e} / \sqrt{tlength E_i}, \quad (4)$$

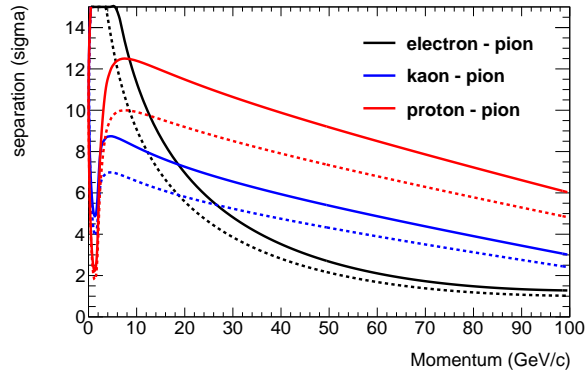


Figure 5: The projected PID separation for a GridPix TPC in ILD for electrons, kaons and protons w.r.t. pions at $\cos \theta = 0$. The continuous lines correspond to an electron PID resolution of 2.4% and the dashed to 3%.

244 where l is the track length and E_i is the expected energy loss for
 245 particle i (electron = e , muon = μ , pion = π , kaon = K , proton = p).
 246 Clearly, the best PID resolution will be reached for the largest track length,
 247 which corresponds to $\cos \theta = 0.85$ in ILD.

248 The ILD parametrisations of the energy loss for different particles as a
 249 function of the momentum were used as given in [6]. They are based on
 250 full simulations of the ILD TPC operated with a T2K gas and running at
 251 atmospheric pressure. The PID separation in numbers of standard deviations
 252 w.r.t. the π hypothesis for the e , K and p is defined as:

$$\text{separation} = |E_i - E_\pi| / \sigma_\pi, \quad (5)$$

253 In Figure 5, the separation of electrons, kaons and protons w.r.t. pions
 254 are shown as a function of the momentum of the particle for projected ILD
 255 electron PID resolutions of 2.4 and 3% at $\cos \theta = 0$. The expected pion-kaon
 256 PID separation for momenta in the range of 2.5-45 GeV/c at $\cos \theta = 0$ is

257 more than $5.5(4.5)\sigma$ for the two resolution scenarios. At a momentum of 100
258 GeV/c the separation is still $3.0(2.0)\sigma$. Protons can be separated from pions
259 for momenta in the range of 2.5-100 GeV/c with more than $6.0(4.8)\sigma$.

260 It is clear from the above that a GridPix Pixel TPC in ILD will provide
261 very powerful particle identification.

262 5. Conclusion and outlook

263 A Time Projection Chamber (TPC) module with 32 GridPix chips was
264 constructed and the performance was measured using data taken in a test
265 beam at DESY in 2021. The analysed data were taken at electron beam
266 momenta of 5 and 6 GeV/c and at magnetic fields of 0 and 1 T.

267 The precise tracking results for the module were presented in part I of
268 the paper [3].

269 The dE/dx or dN/dx resolution for electrons of momenta 5 and 6 GeV/c
270 in the 1 T data for a 1 m track with 60% coverage was measured to be 3.6%
271 for the dE/dx truncation method and 2.9% for the template fit method. This
272 result is impressive and is currently, the best resolution per meter of track
273 length of constructed TPCs running at atmospheric pressure.

274 The single electron efficiency at high hit rates was studied. For hit rates
275 up 1.4 kHz per chip a reduction of at most 0.6% in the relative efficiency was
276 measured.

277 Hit bursts due to highly ionising particles were characterized showing the
278 pattern recognition capabilities of a GridPix Pixel TPC.

279 The resolution in the precision plane as a function of the incident track
280 angle was measured in the $B = 1$ T data using reconstructed circle tracks. It

281 was demonstrated that the resolution in the precision plane is - as expected
282 - independent of the incident angle ϕ within an uncertainty of $16 \mu\text{m}$.

283 The projected particle identification performance of a GridPix Pixel TPC
284 in ILD was presented using the $B = 1 \text{ T}$ test beam results for the measured
285 electron PID resolution. The expected pion-kaon PID separation for mo-
286 menta in the range of $2.5\text{-}45 \text{ GeV}/c$ at $\cos\theta = 0$ is more than 5.5 (4.5) σ for
287 the template fit (dE/dx truncation) method.

288 It is clear that a GridPix Pixel TPC in ILD will provide very power-
289 ful particle identification. At the CEPC collider a Pixel TPC is proposed,
290 because of the precise tracking and particle identification capabilities. The
291 GridPix detector will be further tested and developed for a TPC that could
292 be installed in a heavy ion experiment at the Electron Ion Collider. In the
293 DRD1 collaboration at CERN a GridPix Pixel TPC is also part of the re-
294 search program.

295 **Acknowledgments**

296 This research was funded by the Netherlands Organisation for Scientific
297 Research NWO. The authors want to thank the support of the mechanical
298 and electronics departments at Nikhef and the detector laboratory in Bonn.
299 The measurements leading to these results have been performed at the Test
300 Beam Facility at DESY Hamburg (Germany), a member of the Helmholtz
301 Association (HGF).

302 **References**

- 303 [1] M. Lupberger, Y. Bilevych, H. Blank, D. Danilov, K. Desch, A. Hamann,
304 J. Kaminski, W. Ockenfels, J. Tomtschak, S. Zigann-Wack, To-
305 ward the Pixel-TPC: Construction and Operation of a Large Area
306 GridPix Detector, *IEEE Trans. Nucl. Sci.* 64 (5) (2017) 1159–1167.
307 doi:10.1109/TNS.2017.2689244.
- 308 [2] C. Ligtenberg, A GridPix TPC readout for the ILD experiment at the
309 future International Linear Collider, Ph.D. thesis, Free University of
310 Amsterdam (2021).
- 311 [3] M. van Beuzekom, et al., Towards a Pixel TPC part I: construction and
312 test of a 32-chip GridPix detector, submitted to *Nucl. Instrum. Meth.*
313 *A*.
- 314 [4] T. Behnke, J. E. Brau et al., eds. *The International Linear Collider.*
315 *Technical Design Report. Vol. 4: Detectors.* Linear Collider Collabora-
316 tion, 2013. arXiv: 1306.6329. doi:10.48550/arXiv.1306.6329.
317 URL <https://www.linearcollider.org/>
- 318 [5] LCTPC Collaboration, David Attié et al., A Time Projection Cham-
319 ber with GEM-Based Readout, *Nuclear Instruments and Methods in*
320 *Physics Research. Section A: Accelerators, Spectrometers, Detectors*
321 *and Associated Equipment* 856, 1 (2017), 109–118. arXiv:1604.00935v1,
322 doi:10.1016/j.nima.2016.11.002.
- 323 [6] iLCSoft, *Linear Collider Software*,

324 URL <https://github.com/iLCSoft/MarlinReco/blob/master/Analysis/PIDTools/>,
325 based on version v02-02-01.